Blast Furnace Slag as a Substitute for the Fine Fraction of Aggregates in an Asphalt Mixture

Hugo Alexander Rondón-Quintana, Ph.D.[1]; Juan Carlos Ruge-Cárdenas, Ph.D.[2]; Daniel Francisco Patiño-Sánchez[3]; Hermes Ariel Vacca-Gamez[4]; Fredy Alberto Reyes-Lizcano, Ph.D.[5]; and Márcio Muniz de Farias, Ph.D.[6]

Abstract: Blast furnace slags (BFS) have interesting physical properties and chemical compositions for the production of mastics in asphalt mixtures. However, most of the studies conducted on this material and their applications in asphalt mixtures have been as substitutes for the coarse fraction of natural aggregates (NGA). In the present study, an experimental program was devised to evaluate the effect on the resistance of a hot mix asphalt (HMA), due to the replacement of fine fraction of a NGA by a BFS. The mechanical properties investigated were indirect tensile strengths, resilient modulus, permanent deformation, resistance to fatigue, and moisture damage. Analysis of variance (ANOVA) tests were performed to verify or reject the null hypothesis that the results are statically equal to those of the reference mixture. X-ray diffractometry (XRD) and X-ray fluorescence (XRF) tests were carried out on particles of BFS and NGA. Additionally, the samples were subjected to imaging processing in a scanning electron microscope (SEM). Characterization tests (viscosity, softening point, penetration, and indirect tension) were performed on mixtures made of fine particles (NGA and BFS) and asphalt. The BFS used as fine aggregate tends to generate, in conjunction with asphalt, a material with improved properties of resistance under monotonic and dynamic load. **DOI: 10.1061/(ASCE)MT.1943-5533.0002409.** © *2018 American Society of Civil Engineers.*

Author keywords: Blast furnace slag; Asphalt mixture; Fine aggregate fraction; Resistance under monotonic and cyclic loads; Resistance to moisture damage.

Introduction

Background

Slags can be classified into three categories: ferrous blast furnace slag, nonferrous slag, and incineration slag (Shen and Forssberg 2003). According to Das et al. (2007), blast furnace slags (BFS) are inorganic materials whose typical composition is silica (30–35%), calcium oxide (28–35%), magnesium oxide (1–6%), and Al_2O_3/Fe_2O_3 (18–25%). This material is formed when iron ore, coke, and flux (either limestone or dolomite) are melted together in a furnace. When the metallurgic casting process is complete, the lime in the flow has been chemically combined with the aluminates and silicates of mineral ash and coke, generating the BFS (FHWA 2008; Marriaga and Claisse 2011). According to the NSA (2006), the slag from the blast furnaces is slowly cooled outdoors [air-cooled blast furnace slag (ACBFS)] or quickly cooled by applying jets of cold water (expanded slag). ACBFS is used in the construction mainly as aggregate (concrete and fillers, among others), while expanded slag is generally used in cement production. Expanded slag, because of its increased porosity and reduced weight compared to ACBFS, is also used in the manufacture of concretes and light masonry (Van Oss 2003).

According to Okumura (2013), Proctor et al. (2000), and Airey et al. (2004), the annual production of BFS in the United States, Japan, and the UK is 13, 24.3, and 4 million tons, respectively. For each ton of iron produced, an amount of BFS between 220 and 370 kg (Proctor et al. 2000) or 340 and 421 kg (Das et al. 2007) is generated. In Colombia, the iron production was estimated at 710,047 tons for 2013 (UPME 2014) and increased to 901,736 tons during 2015 (HERALDO 2016), from which an annual production of approximately 2×10^5 tons of BFS can be estimated. The conventional method of slag disposal is transporting and depositing the material in open heaps and landfills. This generates an environmental problem because they occupy spaces in landfills, besides wasting a material that can be reused. According to Nouvion et al. (2009), using BFS could generate the following benefits: (1) reducing the use of natural aggregates, preventing additionally the release of pollutants into the air, water, and soil during the processing of such materials, and (2) reducing energy consumption from the exploitation of natural aggregates.

BFS have been used widely in the world for over a century as fertilizers (Geiseler 1996), in road construction (Houben et al. 2010),

[1]Full Professor, Faculty of Environment and Natural Resources, Universidad Distrital Francisco José de Caldas, Avenida Circunvalar sede Vivero UD, Bogotá, DC 110131, Colombia (corresponding author). Email: harondonq@udistrital.edu.co; harondon2012@hormail.com

[2]Full Professor, Civil Engineering Program, Faculty of Engineering, Universidad Piloto de Colombia, Carrera 9 No. 45A-44, Bogotá, DC 110231, Colombia. Email: juan-ruge@unipiloto.edu.co

[3]Assistant Professor, Technology Faculty, Universidad Distrital Francisco José de Caldas, Cl. 68D Bis A Sur N° 49F - 70, Universidad Distrital, Bogotá, DC 111931, Colombia. Email: dfpatinos@correo.udistrital.edu.co

[4]Associate Professor, Dept. of Civil Engineering, Faculty of Engineering, Pontificia Universidad Javeriana, Carrera 7 No. 40-62, Bogotá, DC 110231, Colombia. Email: vacca@javeriana.edu.co

[5]Full Professor, Dept. of Civil Engineering, Faculty of Engineering, Pontificia Universidad Javeriana, Carrera 7 No. 40-62, Bogotá, DC 110231, Colombia. Email: fredy.reyes@javeriana.edu.co

[6]Full Professor, Faculty of Technology, Universidade de Brasília, Campus Universitário Darcy Ribeiro, 70910-900, Brasília-DF, Brazil. Email: muniz@unb.br

Note. This manuscript was submitted on July 24, 2017; approved on March 2, 2018; published online on July 12, 2018. Discussion period open until December 12, 2018; separate discussions must be submitted for individual papers. This paper is part of the ***Journal of Materials in Civil Engineering***, © ASCE, ISSN 0899-1561.

in soil remediation, and in the preparation of materials such as glass ceramic, silica gel, and bricks, among others (Das et al. 2007). However, perhaps its best use is in the production of cement (Shi 2004; Das et al. 2007; Abu-Eishah et al. 2012; Sorlini et al. 2012), because this type of slag (Das et al. 2007) (1) contains little iron, has a high content of calcium oxide, and is similar composition to clinker; (2) is a material that can be used safely together with clinker and gypsum; (3) can be used safely in the production of cement as a result of its low content of iron, ; (4) helps developing properties in cement such as low heat hydration, good long-term resistance, and acid resistance; and (5) allows cost reduction in the cement industries. Additionally, Shi (2004) mentions that BFS exhibits cementitious properties. Regarding the use of BFS in construction projects, there are few environmental concerns, since slag's components are tightly bonded to its matrix and would not leach so easily.

Airey et al. (2004) report that BFS produces an aggregate with a rough surface texture and relatively high porosity (typical absorption between 3 and 7%) that results in good adhesion with bituminous binders. However, these properties imply greater consumption of bitumen to produce an asphalt mixture (Airey et al. 2004; FHWA 2008), resulting in an increase of costs. Nevertheless, this higher cost could be offset by the higher productivity (volume by mass) of BFS as aggregate due to the lower unit weight (Noureldin and McDaniel 1990; Zarei and Reza 2015) of the mixture. Some conclusions reported by the FHWA (2008) are the following: (1) The surface layers using BFS as aggregates have good resistance to friction [because of its angular form, they generate a high friction angle between 40 and 45° (Van Oss 2003; Noureldin and McDaniel 1990)], good resistance against stripping, and high stability. However, the impact resistance is not very high, and the material can be crushed under heavy traffic conditions [Los Angeles abrasion is between 35 and 45% (Noureldin and McDaniel 1990)]. Therefore, these materials are more suitable as aggregates to be applied in the surface courses of low-traffic pavement (ASA 2002). (2) The variability in the production process of iron may lead to high dispersion in the physical properties (gradation, specific gravity, absorption, and angularity). (3) Although resistance to abrasive wear and tear of BFS in the Los Angeles machine is not particularly favorable (as sharp edges break), the field performance has been satisfactory. For this reason, this test has been removed from some standard specifications to characterize BFS. (4) BFS have good compatibility with asphalt, which helps developing good adherence. (5) Being a porous material compared with conventional natural aggregates, it may require longer drying time in production plants of asphalt mixtures.

Problem Statement

The mastic in asphalt mixtures is responsible for providing stiffness, cohesion, adhesion between the binder and the stone aggregate, shear strength, resistance to aging, and resistance to moisture damage (Liao and Chen 2011; Yiqiu et al. 2012; Dan et al. 2014; Davis and Castorena 2015; Kuity and Das 2015; Tenza-Abril et al. 2015; Veytskin et al. 2015). BFS have interesting physical properties for the production of mastics in asphalt mixtures, among which the following characteristics are emphasized: porosity and good compatibility with asphalt to improve adhesion, low specific weigh, rough surface texture and angular form, and chemical composition with high contents of CaO and SiO_2 (similar to the composition of clinker and cement). Most of the studies conducted on this material and their applications in asphalt mixtures have been as substitutes for the coarse fraction of natural granular aggregates (NGA), perhaps because the size of BFS particles is predominantly coarse, among others. However, the BFS are used widely in the production of cement, and for such reason, large quantities of them are obtained in very fine particles, while the filler obtained from NGA requires large energy consumption during its exploitation and production procedures. Therefore, another possible practical application of the BFS would be as filler in HMA. Few studies have been performed to evaluate the potential use of BFS as filler or fine granular aggregate of asphalt mixtures. Some of them have been performed in the analysis of cold asphalt mixtures and have blended the BFS with other types of fillers (e.g., Nassar et al. 2016; Al-Hdabi and Al Nageim 2017). Other studies have used steel slags (SS) for this purpose (e.g., Li et al. 2017).

Objective

The objective of the present study was to evaluate the effects of using blast furnace slag (BFS) as substitutes of the fine particles of a natural aggregate (NGA) in the manufacture of hot mix asphalts (HMA), to determine if such replacement produces statistically significant improvements in the resistance of the mixture against moisture damage, permanent deformation, and fatigue, under cyclic loadings.

General Methodology

Initially a series of tests were carried out for the characterization of the granular materials (BFS and NGA) and the asphalt binder, followed by the design of asphalt mixtures with partial substitution of NGA by BFS. Asphalt cements with penetration grades CA 60-70 and PG 58-22 were used as binders for the manufacture of the mixes. The grain size distribution of the aggregates follows the prescription of INVIAS (2013) for asphalt concrete HMA-19 (maximum nominal size particle of 19 mm) due to the fact that these are the asphalt and the mixture types most commonly used in Colombia for the construction of asphalt layers.

The resistance of these mixtures was evaluated under monotonic loading using the Marshall test [AASHTO T245 (AASHTO 2015a)] and indirect tension test [ASTM D6931 (ASTM 2017b)] in samples in which the fine fraction of the NGA was replaced by BFS. These initial experiments were carried out to define the mixture with best performance under monotonic load, to later investigate its properties under cyclic loading (resilient modulus—EN 12697-26 (BSI 2005b), resistance to permanent deformation—EN 12697-25 (BSI 2000), and fatigue—EN 12697-24 (BSI 2005a) and moisture damage (ASTM D6931). In addition, viscosity [ASTM D4402 (ASTM 2015)], softening point [ASTM D36 (ASTM 2006)], penetration [ASTM D5 (ASTM 2013)], and indirect tensile (ASTM D6931) tests were performed on mastics produced using NGA and BFS as fillers.

To evaluate whether the NGA substitution by BFS produced statistically significant effects on the HMA mix properties, an analysis of variance (ANOVA) with F-test was performed with a confidence level of 95%.

Materials and Methods

Material Characterization

Slags are highly heterogeneous materials as to forms and particle sizes, chemical composition, texture, specific gravity, wear and tear resistance, and porosity among others, which implies complex characteristics and properties (Akbarnejad et al. 2014). This is illustrated in Fig. 1, which shows some particles that prevail in the BFS used in this study. Some of them have a shiny black surface, and they are the ones that are present in greater amounts in the BFS (approximately 65% with respect to the total number of particles); when

Fig. 1. Slag particles (size between 19 and 25.4 mm diameter). (Images by authors.)

crushed, the particles show an internal grayish color. Additionally, they have a rigid, hard, and bulk consistency similar to that of natural aggregates (NGA), although they are much more porous (for example, on average, BFS and NGA particles of 25.4 mm (1-in.) diameter have an average mass of 32 and 35 g, respectively). On the contrary, the other types of particles have a light green surface color and they are easy to abrade (even with the hands), are lightweight, have a light green hue, and float in the water (a particle with a 25.4 mm (1-in.) diameter has a mass of about 9 g on average).

Table 1 [AASHTO T84 (AASHTO 2000); AASHTO T85 (AASHTO 1991b); UNE 14613 (AENOR 2000)] and Table 2 [AASHTO T228 (AASHTO 2004); AASHTO T316 (AASHTO 2013); ASTM D-36 (ASTM 1995); ASTM D-113 (ASTM 1999); ASTM D2872-12e1 (ASTM 2012); NLT 181 (Normas NLT 1988)] present the values obtained from the characterization tests performed on the aggregates (NGA and BFS) and on AC 60–70 asphalt, respectively. The BFS used was of ACBFS type produced by Acerías Paz del Río (Nobsa, Boyacá, Colombia). This company produces monthly 28,000 tons of pig iron and 22,000 tons of BFS and steel slags (Ucrós 2009). The NGA used is a limestone-type mineral aggregate.

It is observed in Table 1 that by decreasing the particle size of BFS, the specific gravity increases while absorption decreases. This is due to its heterogeneous nature and because part of the voids are excluded during the mechanical fracturing process executed on coarse particles to obtain the fine particles. Based on the results of Micro-Deval [AASHTO T327 (AASHTO 2005)] and 10% of fines [DNER-ME 096 (DNER 1998)], it is concluded that this BFS presents good resistance to abrasion by friction between particles and to crushing under a monotonic load, respectively. However, as reported in the reference literature, BFS are materials that generally have low resistance to wear and tear by impact abrasion on the Los Angeles machine [AASHTO T96 (AASHTO 1991a)]. It is also observed that the material has particles with ideal shapes (rounded angular faces fractured with very little content of elongated and flattened particles) [ASTM D5821 (ASTM 2001); NLT 354 (NLT 1991)]. This should help to develop a good granular skeleton after the compaction processes of asphalt mixtures, as well as to resist static, dynamic, or impact loads. The fine particles have no clay content, organic matter, or dust that could generate decreased adhesion between the aggregate and the asphalt, and reduced strength and durability of the mixture by excess of fines or contaminants [AASHTO T176 (AASHTO 2002); ASTM D4318 (ASTM 2000); AASHTO T21 (AASHTO 2015b); T220 RMS 12.495 (Transport Roads and Maritime Services 2012)].

On the other hand, screening tests based on X-ray diffractometry (XRD) and X-ray fluorescence (XRF) were performed on the fine fractions of the BFS and NGA to obtain their mineralogical and chemical compositions. The detailed description of the execution of these tests can be found in Zhang et al. (2003), Chipera and Bish (2001), Moore and Reynolds (1997), and Beckhoff et al. (2006). Particles of both materials were also subject to observation in the scanning electron microscope (SEM) to determine the predominance and diameter of macropores and micropores in the samples [details in Reed (2005)]. Table 3 presents the mineralogical composition of the samples analyzed (NGA and BFS) and the chemical compositions of BFS reported by several researchers. It is observed that the predominant mineral in both samples is quartz [silica (SiO_2)]. This result is consistent with that obtained in the XRF test (Table 4) in which the predominant chemical component is silica (SiO_2). However, the main difference lies in the greater amount of CaO in the BFS and the presence of some clay minerals in the NGA. It is further concluded that the analyzed BFS sample is composed mainly of silica, calcium oxide (CaO), and aluminum oxide (Al_2O_3, 92.76%), while the NGA sample is composed mainly of silica and Al_2O_3 (86.86%). Oxides SiO_2 and Al_2O_3 are pozzolanic compounds, which in very fine particle sizes can

Table 1. NGA and BFS characterization

Test	Method	NGA	BFS
Specific gravity/absorption [19 mm (¾ in.)]	AASHTO T84-00	2.51/1.66%	1.91/3.75%
Specific gravity/absorption [9.5 mm (⅜ in.)]	AASHTO T85-91	2.49/1.70%	1.97/3.33%
Specific gravity/absorption (No. 4)		—	2.11/2.73%
Specific gravity/absorption (No. 40)		—	2.26/2.65%
Specific gravity/absorption (No. 80)		—	2.36/2.25%
Specific gravity/absorption (No. 200)		—	2.51/1.90%
Specific gravity of sands and fines/adsorption	—	2.50/1.50%	—
Abrasion in Los Angeles machine, 500 revolutions	AASHTO T96-02	24.6%	49.2%
Micro-Deval	AASHTO T327-05	22.3%	29.2%
10% of fines (dry resistance)	DNER-ME 096-98	115 kN	123 kN
Fractured particles: 1 face	ASTM D5821-01	87%	92%
Fractured particles: 2 faces		80%	88%
Impurities content	UNE 14613: 2000	0%	0%
Plasticity index	ASTM D4318-00	No plastic	No plastic
Flattening index	NLT 354-91	9.5%	5.62%
Elongation index		9.5%	10.62%
Sand equivalent test	AASHTO T176-02	76%	—
Iron unsoundness	T220 (RMS 12.495)	—	Free

Table 2. General properties of AC 60-70

Test	Method	Unit	Value
Tests on the original AC			
Penetration (25°C, 100 g, 5 s)	ASTM D5	0.1 mm	62.5
Penetration index	NLT 181/88	—	−0.7
Softening point	ASTM D36-95	°C	52.5
Absolute viscosity (60°C)	ASTM D4402	Poises	1,750
Specific gravity	AASHTO T228-04	—	1.012
Viscosity to 135°C	AASHTO T316	Pa-s	0.36
Ductility (25°C, 5 cm/min)	ASTM D113	cm	>105
Tests on the residue of AC after the RTFOT			
Mass loss	ASTM D2872	%	0.47
Penetration (25°C, 100 g, 5 s) of the original penetration	ASTM D5	%	72
Increase on the softening point	ASTM D36-95	°C	5

Table 3. Chemical composition of BFS and NGA

			Others BFS					
Component	BFS	NGA	Emery (1982)	Jones (1982)	León et al. (2009)	WSDOT (2015)	Al-Hdabi and Al Nageim (2017)	Nassar et al. (2016)
CaO (%)	30.83	1.09	36–45	40	43.3	32–45	40.37	41.42
SiO_2 (%)	52.03	79.00	33–42	36.8	25.5	32–42	37.47	35.65
Al_2O_3 (%)	9.90	7.86	10–16	16	17	7–16	4.76	11.21
P (%)	—	—	—	—	2.3	—	—	—
MgO (%)	0.82	2.34	3–16	5.4	1.45	5–15	3.65	6.89
Na_2O (%)	0.65	1.82	—	—	1.4	—	2.55	0.28
SO_3 (%)	0.48	—	1–3	0.4	1	0.4–2	—	2.43
FeO (%)	—	—	0.3–0.2	0.2	—	—	—	—
Fe (%)	—	—	—	—	0.5	—	—	—
Fe_2O_3 (%)	1.52	3.70	—	—	0.71	0.1–0.75	0.15	0.26
MnO (%)	1.26	—	0.2–1.5	0.5	—	0.2–0.8	—	0.60
TiO_2 (%)	0.98	0.44	—	0.3	—	—	—	0.63
K_2O (%)	0.86	1.17	—	0.4	0.14	—	0.62	0.64
Ba (%)	0.21	—	—	—	—	—	—	—
P_2O_5 (%)	0.06	0.11	—	—	—	—	—	—
Cr (%)	0.12	—	—	—	—	—	—	—
Others (%)	0.24	—	—	—	—	—	—	—

develop self-hardening properties and do not need to be activated with water or lime (Misra et al. 2005). This pozzolanic property can increase the resistance to moisture damage of asphalt mixtures (Nassar et al. 2016). Also, these two oxides can improve asphalt-aggregate surface adhesion and internal cohesion in the asphalt mixture (Modarres and Rahmanzadeh 2014). In addition, the presence of high content of quartz in the BFS suggests that it can develop high strength and interlocking in the mineral skeleton. This is an important aspect to be taken into account, since the BFS used in the study presents a higher content of quartz compared to those studied previously (Table 3). According to Modarres and Rahmanzadeh (2014), Anderson and Goetz (1973), and Muniandy et al. (2013), the CaO is alkaline, which contributes to increase the aggregate-asphalt adhesion, and improves the resistance to moisture damage and stripping. Muniandy et al. (2013) reported that SiO_2 is a material of high hardness and mechanical strength, and that Al_2O_3 can improve adhesion between aggregate and asphalt (mainly because of the great affinity of this chemical component with the oil fractions of asphalt), increasing the resistance of the mixtures to rutting. Guo et al. (2016), using molecular dynamics (MD) simulation, found that the interfacial energy and work of adhesion of the four asphalt components (saturates, aromatics, resins, and asphaltenes) with mineral aggregates is greater when these are composed mainly of CaO. A similar conclusion was obtained by Li et al. (2016), also using MD simulation; however, in this study, the interaction capability and interfacial energy ranking of oxides evaluated with the asphaltenes was as follows: MgO > CaO > Al_2O_3 > SiO_2.

The preparation of samples of BFS and NGA for the SEM observation was preceded by the selection of different particles, to obtain a statistically reliable result. In the case of the BFS, the selected particles were five of green coloration, three of black coloration, and one of white coloration (because the white coloration was scarcer

Table 4. Mineral percentages in the BFS and NGA samples (XRD test)

Sample	Mineral	Mass (%)
BFS	Quartz	58.9
	Cristobalite	18.1
	Boehmite	12.8
	Calcite	4.8
	Natrolite	5.3
NGA	Quartz	61.00
	Albite	25.05
	Illita	5.28
	Chlorite	8.67

Table 5. Porosities calculated values

Particle type	Porosity (%)	Pore diameter (μm)
	NGA	
G1	0.6	6.0
G2	20.8	27.1
G3	13.9	10.4
G4	6.5	36.4
G5	2.3	11.0
G6	0.98	7.9
G7	0.86	7.8
	BFS	
Green	63	82.6
Black	9	27.5
White	50	30.3

in the analyzed population). NGA particles were chosen in seven groups (G1–G7, see Table 5), which had different lithological characteristics and did not share characteristics of size, color, and/or sphericity. Observations were performed using a Field Emission Scanning Electron Microscope (FESEM) JEOL JSM 6700F (JEOL, Tokyo, Japan) SEM with an acceleration voltage of 20 kV in high vacuum at a working distance of approximately of 15 mm. The micrographs were taken with a backscattered electron detector (BSE). Several images of each grain were taken with a 30x magnification. Fig. 2 shows an example of the surface porosity of the NGA and BFS particles, and Table 5 shows the average porosity and the average pore diameter measured in the samples. Based on Fig. 2, BFS particles exhibit different morphology compared to NGA. High amounts of large pores can be distinguished clearly on the surface of the BFS. It is observed that the analyzed BFS particles have higher porosity and pore diameter than the particles of NGA, which explains why BFS can absorb a greater amount of asphalt. Additionally, the relationship between the particle size of BFS and the absorption of asphalt should be directly proportional, since the higher porosity and pore dimensions obtained in the test would generate a coarse aggregate with lower specific gravity, higher absorption (as reported in Table 1), and higher fracture probability under mechanical load.

Marshall Tests

To evaluate the reproducibility of the results, five Marshall samples (101.6 mm in diameter and 63.5 mm in height) were compacted applying 75 blows per face for each asphalt percentages of 4.5, 5.0, 5.5, and 6.0%, using the grain-size distribution presented in Fig. 3 and NGA as aggregate. Prior to the mixture and compaction procedures of the samples, the aggregate was dried in the oven for 24 h at a temperature of 105°C and then hot bitumen was added. The temperatures of the samples for compaction and for mixing in the laboratory were 140 and 150°C, respectively. These values were obtained based on the criteria established by the ASTM D6925 (ASTM 2009) specification, in which the viscosity required to obtain mix and compaction temperatures of HMA mixtures are 85 $\pm$ 15 Saybolt Furol (SSF) [0.17 Pa · s (170 cP)] and 140 $\pm$ 15 SSF [0.28 Pa · s (280 cP)], respectively. Bulk specific gravities and volumetric composition were calculated in accordance with ASTM D2726 (ASTM 2017a). Marshall tests (AASHTO T245) were performed on these samples (HMA-19 of control, BFS = 0%) to obtain their volumetric indices (mainly, air voids in volume – Va) and resistance under monotonic load (stability – S, flow – F, and S/F ratio). This test was performed additionally on samples made with asphalt contents of 5.0, 5.5, 6.0, and 6.5%, and using BFS as follows (five samples were tested for each replacement of NGA by BFS and asphalt content):

1. BFS = 6%, replacing only the material on the bottom.
2. BFS = 12.5%, replacing the bottom and the sieve No. 200.
3. BFS = 19.5%, replacing the bottom and sieves No. 80 and No. 200.
4. BFS = 31%, replacing sieves No. 40, No. 80, and No. 200.
5. BFS = 37.5%, replacing the bottom and sieves No. 40, No. 80, and No. 200.

Indirect Tensile Strength Tests

Indirect tensile tests [ASTM D4867 (ASTM 2014)] were carried out on the control asphalt mixture (HMA-19, BFS = 0%) and the other two mixtures with substitution of NGA by BFS, which presented the best performance in the Marshall test. Six samples of each mixture were tested, three under a dry condition (D) and three in wet condition (W), with air void percentages ranging from 7 $\pm$ 1% as recommended by the ASTM D4867 specification. With the test results, the resistance to moisture damage parameter TSR was calculated using the ratio of indirect tensile strengths (W/D). The samples to be tested under wet conditions were placed in a saturation vacuum with a pressure of approximately 6.7 kPa during 5 min, and then the specimens were submerged for another

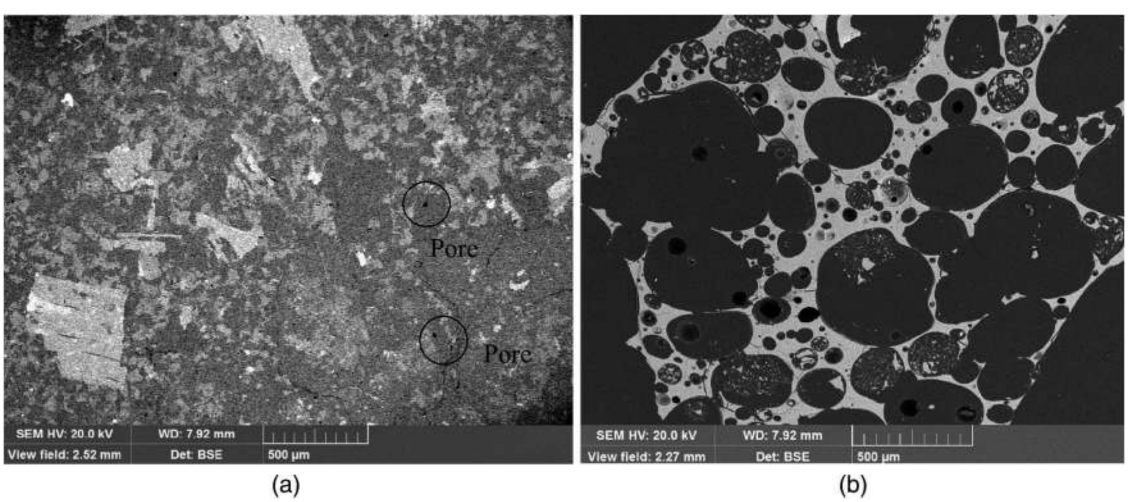

Fig. 2. SEM observation of (a) NGA; and (b) BFS.

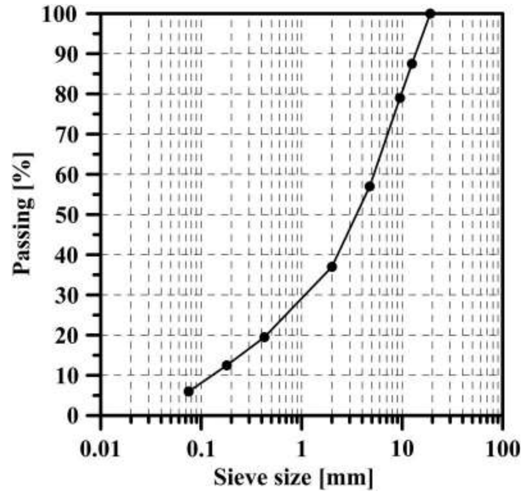

Fig. 3. Particle size distribution of HMA-19.

10 min in a water bath. Thereafter, the samples were submerged in a water bath at 60°C for 24 h. Prior to the indirect tensile tests, the samples were submerged in water at 25°C for 2 h.

Resilient Modulus Tests

On the control asphalt mixture (HMA-19, BFS = 0%) and the mixtures with the substitution of NGA by BFS that presented the best performance in the Marshall test were performed resilient modulus tests (EN 12697-26) under three temperatures (10, 20, and 30°C) and three loading frequencies (2.5, 5.0, and 10.0 Hz). For each test temperature, the Marhall specimens (4 in. in diameter and 2.5 in. in height) were placed in the climatic chamber for 4 h before testing. Resilient modulus tests were performed on nine samples (three for each temperature) using Nottingham asphalt tester (NAT) equipment. The amplitude of the load was controlled to keep a deformation level lower than 50 microstrains in accordance with EN 12697-26 requirements.

Permanent Deformation Tests

Permanent deformation tests (EN 12697-22) under repeated square-wave load with a stress of 100 kPa, test temperature of 40°C, and 3,600 load cycles (N) were performed on the Marshall specimens used in the resilient modulus tests. NAT equipment was used to perform the tests. Prior to the tests, the specimens were preconditioned in the thermostatic chamber at 40°C during 4 h. Then, Marshall samples were preloaded under 10 kPa during 10 min. After the preloading time, the stress of 100 kPa was applied in 3,600 pulses with 1 s of load followed by a rest period of 1 s (frequency of 0.5 Hz).

Fatigue Resistance Tests

Indirect tensile fatigue tests (ITFT), according to UNE-EN 12697-24, controlled stress procedure were conducted on the control mixture and the mix with BFS that presented the best performance under monotonic (Marshall and indirect tensile tests) and dynamic loading conditions (resilient modulus and resistance to permanent deformation). Each fatigue test was performed using 15 samples (three replicates for each of the five constant stress levels applied ranging from 100 to 600 kPa). Prior to testing, the specimens were placed in the thermostatic chamber and exposed to 20°C during 4 h. All fatigue tests were performed under a temperature of 20°C using NAT equipment, Marshall specimens (4 in. in diameter and 2.5 in. in thickness), and repetitive applications of compressive controlled-load in a haversine waveform with load time of 0.1 s and rest time of 0.4 s. The fatigue resistance was determined as the total number of load applications that caused the complete fracture of the specimen (N_f).

Tests Performed on Mixtures of Fine Aggregates and Asphalt

To understand the results from the previous experimental phases, the following tests were performed on two mastics of fine aggregates (only NGA or only BFS) with asphalt: viscosity at 135 and 150°C (Brookfield viscometer was used to measure apparent viscosity, ASTM D4402), softening point (ASTM D36), and penetration (ASTM D5). Both mixtures were produced taking into account the best behavior obtained in the previous experimental phases. Therefore, the composition of the fine aggregate particles was 52 and 48% of material retained in sieves No. 200 and the bottom, respectively. The asphalt content used was 5.0% with respect to total mass of the mixture (ratio between fine aggregate and asphalt of 2.5). A mechanical mixer was used to blend the filler and asphalt binder at the established mixing temperature of 150°C. Prior to mixture with the bitumen, the aggregates were dried in the oven for 24 h at a temperature of 105°C. The mixture was made until a homogeneous distribution between both materials was reached. Five replicate samples were prepared and tested to evaluate each property. Additionally, indirect tensile tests (ASTM D6931) were performed on two samples produced with the same two mixtures and fine aggregate composition mentioned previously. However, to mix adequately the fine aggregate with the asphalt and to perform

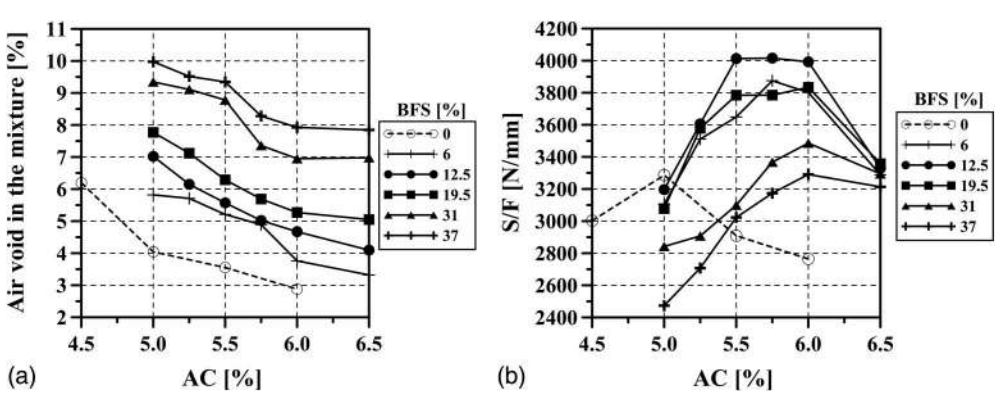

Fig. 4. Marshall test. Substitution of the fine fraction of NGA by BFS: (a) air void; and (b) S/F ratio.

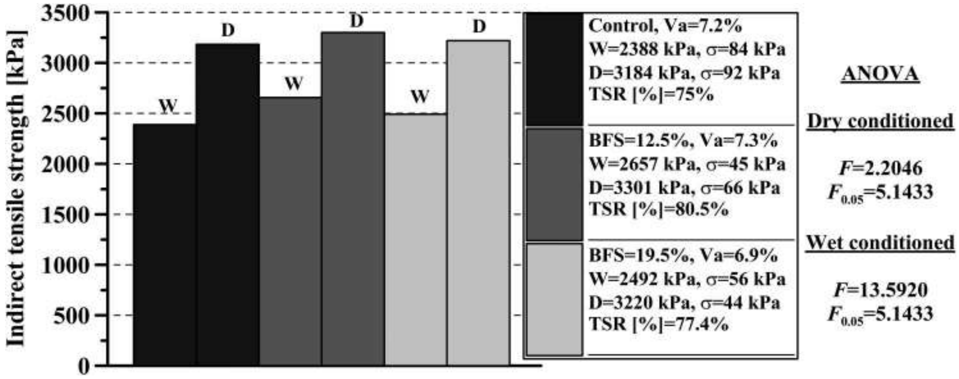

Fig. 5. Indirect tensile test. Va = air void; and σ = standard deviation.

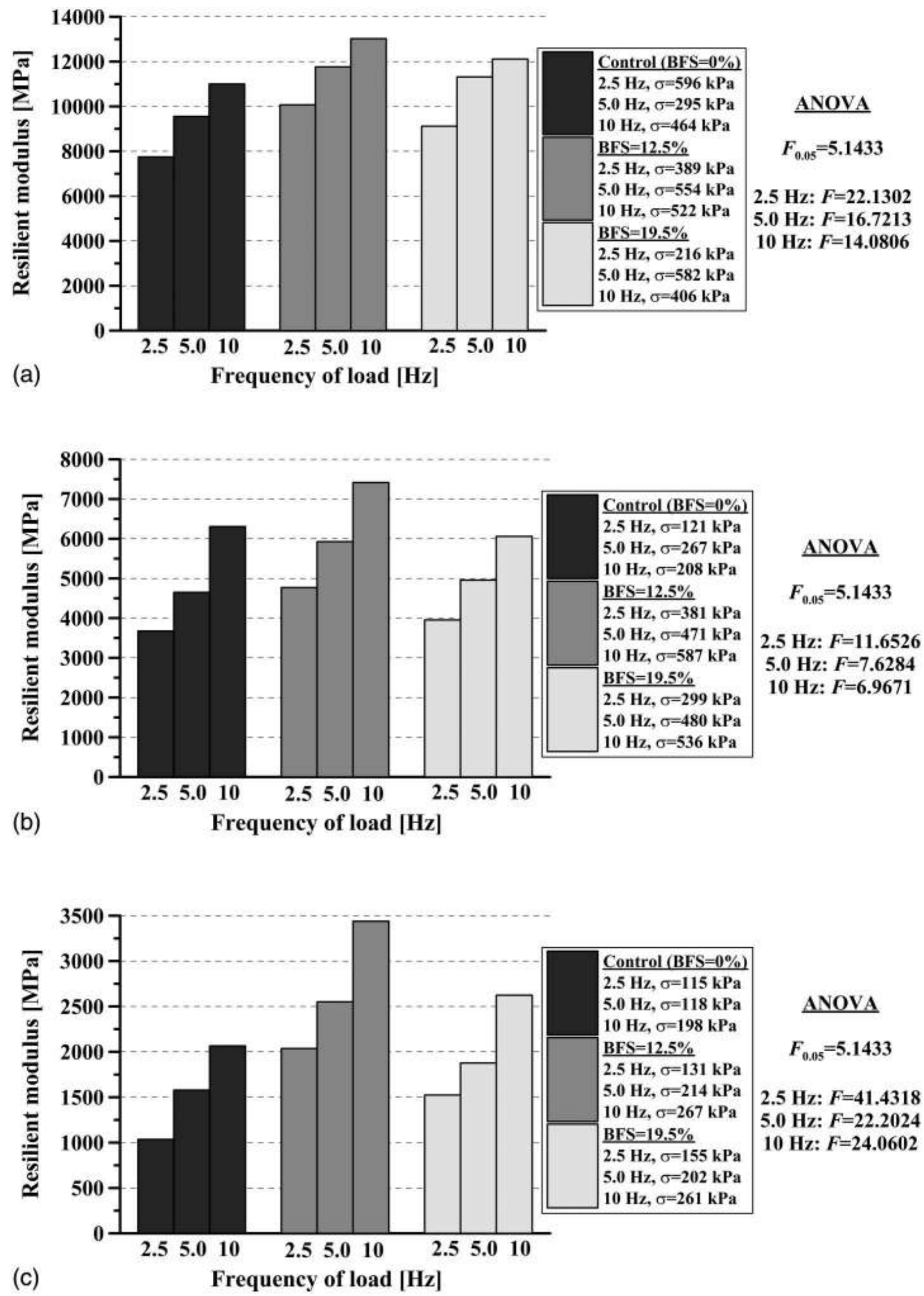

Fig. 6. Resilient modulus: (a) 10°C; (b) 20°C; and (c) 30°C.

Marshall specimens of 1,200 g, it was necessary to increase the amount of bitumen. The asphalt content was 12.5%. Three samples of each mixture were tested under dry conditions (D) and the other three in wet conditions (W).

Results

Resistance under Monotonic Load

Fig. 4 shows the results of the Marshall test executed on the asphalt mixture of control (HMA-19, BFS = 0%) and on the mixtures for which some of the finer fraction of NGA was replaced by BFS. In general terms it was observed that:

1. When replacing the fine fraction of NGA by BFS, the air voids in the mixture increased, and these increments were greater when the BFS content increased [Fig. 4(a)].
2. When the finer particles of NGA were replaced by BFS in proportions BFS = 6, 12.5, and 19.5%, the magnitude of the stability/fluency (S/F) relationship [Fig. 4(b)] was similar to the maximum reached by the mixture of control BFS = 0% (asphalt content of 5%). This was achieved, despite the fact that the mixture with BFS has greater air void content (approximately between 3 and 4% higher). If the asphalt content was increased by 0.25 and 0.5% (asphalt content of 5.25 and 5.5%), the ratio under monotonic loading (S/F) increased in 9.7% (320 N/mm) and 22.1% (726.3 N/mm), respectively, when the fine fraction of NGA was replaced at a ratio of BFS = 12.5%. In the case of substitution at ratios of BFS = 6 and 19.5%, the increments were of 6.9% (225.1 N/mm), 8.9% (292.5 N/mm) and 11% (363 N/mm), 15.2% (498.4 N/mm), respectively.
3. In summary, the best performance of replacement of NGA by BFS was reached when particles with a size of 0.18 mm or less (BFS = 12.5%) were substituted.

Therefore, and taking into account the results presented in Fig. 4, mixtures replacing the fine fraction of NGA by BFS in proportions of BFS = 12.5 and 19.5% were chosen to perform indirect tensile tests and dynamic tests. Also, an asphalt content of 5.25% was chosen for both mixtures (a higher content of asphalt was not chosen to not significantly raise the cost of the mixture). For comparison, the control mixture (HMA-19, BFS = 0%) in these tests will be the one prepared with an asphalt content (AC) of 5%.

Fig. 5 shows the results of the indirect tensile tests. It was observed that the BFS = 12.5 and 19.5% (AC = 5.25%) mixtures developed higher indirect tensile strength under wet conditions and greater moisture damage resistance (TSR) with respect to the control mixture (BFS = 0%, AC = 5%). Besides, ANOVA analysis showed that the BFS had a significant effect on the wet conditioned indirect tensile strength (W) with a confidence level of 95% (see Fig. 5, $F > F_{0.05}$). However, for the case of dry conditioned samples (D), the null hypothesis that the strengths are equal cannot be rejected.

Resilient Modulus, Permanent Deformation, and Resistance to Fatigue

Test results of the resilient modulus are presented in Fig. 6. BFS = 12.5 and 19.5% mixtures tend to have higher stiffness under cyclic loading than the control HMA (BFS = 0%). The highest stiffness is developed by the mixture that substitutes the fine fraction of NGA at a ratio of BFS = 12.5% (particles smaller than 0.18 mm). This mixture shows stiffness on average 24, 25, and 75% higher than that of control for test temperatures of 10, 20, and 30°C, respectively. In the case of the BFS = 19.5% mixture, this average increment in stiffness oscillates between 16, 3, and 31%, respectively. ANOVA analysis shows that the BFS have a significant effect on the resilient modulus for each temperature evaluated (Fig. 6).

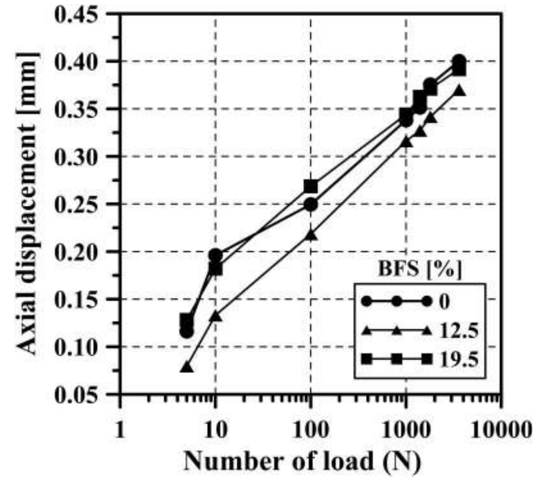

Fig. 7. Permanent deformation.

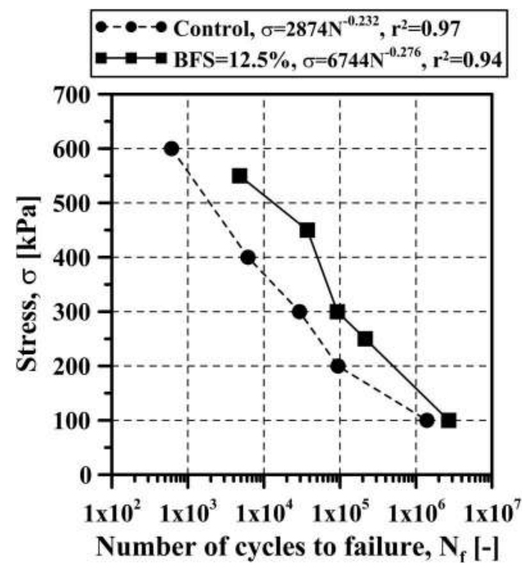

Fig. 8. Fatigue test result.

Table 6. Viscosity values

Material	Viscosity at 135°C (cP)	Viscosity at 150°C (cP)
Asphalt	360	102
Asphalt + NGA	472.5	285.4
Asphalt + BFS	605.7	442.0

Table 7. Penetration and softening point values

Material	Softening point (°C)	Penetration (mm/10)
Asphalt	52.5	62.5
Asphalt + NGA (mix)	58.2	42.2
Asphalt + BFS (mix)	61.7	37.6

J. Mater. Civ. Eng., 2018, 30(10): 04018244

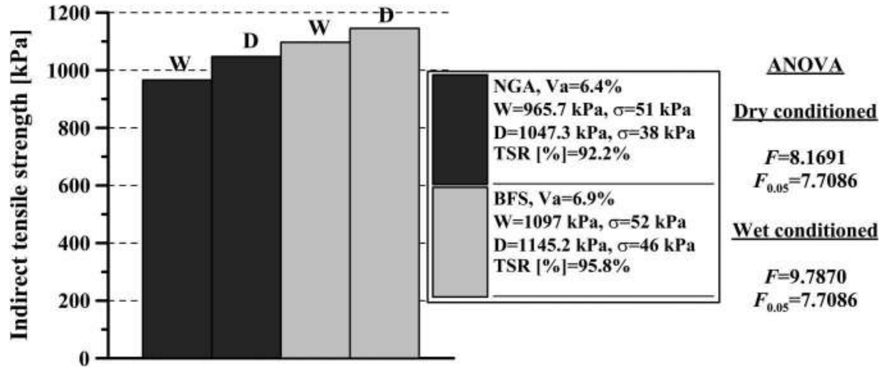

Fig. 9. Indirect tensile test performed on Marshall specimens with fine aggregates of NGA and BFS.

The permanent deformation results are presented in Fig. 7. The greater resistance to permanent deformation under cyclic loading was achieved by the mixture that substituted the fine fraction of NGA at a proportion of BFS = 12.5%. This result is consistent with those obtained in Fig. 6 for the case of the resilient modulus. However, for the case of the BFS = 19.5% mixture, the accumulation of permanent deformation is similar to that of the control mixture (BFS = 0%), mainly because of its greater air void content [Fig. 4(a)]. Therefore, to perform the fatigue tests, the mixture with BFS = 12.5% was chosen. ANOVA analysis for permanent deformation test was calculated at N = 3,600 (final load cycle). It showed that the BFS had a significant effect on the axial displacement measured ($F = 49.9288 > F_{0.05} = 5.1433$).

Fig. 8 shows that HMA with BFS = 12.5% developed higher resistance to fatigue in comparison to control mixture. In this test, the ANOVA analysis was calculated for the stress levels of 100 and 300 kPa, showing that the BFS had a significant effect on the fatigue resistance ($F = 17.4723 > F_{0.05} = 7.7086$ and $F = 78.8449 > F_{0.05} = 5.1433$ for 100 and 300 kPa, respectively).

Tests Performed on Mixtures of Fine Aggregates and Asphalt

Penetration test measures the consistency of the asphalt or asphalt mastics and indirectly is an indicator of stiffness. Viscosity and softening point of asphalt mastic are directly associated with shearing deformation resistance and high temperature stability, respectively (Cheng et al. 2015, 2016). Tables 6 and 7 show the results of viscosity, penetration, and softening point tests performed on the asphalt and the mastics made with the asphalt and fine aggregates of NGA and BFS (asphalt, asphalt + NGA, and asphalt + BFS, respectively). BFS as fine aggregate provided the best behavior for asphalt mastic, since it enhanced the stiffening effect and improved high-temperature susceptibility (lower penetration and greater viscosity and softening point) compared with NGA.

The TSR parameter of indirect tensile test is directly correlated to the susceptibility of the mixes to the action of water. Additionally, the tensile resistance is correlated also with adherence properties between aggregate and asphalt. Fig. 9 shows the results of the indirect tensile tests performed on Marshall specimens produced with fine aggregates (NGA and BFS) and 12.5% of asphalt. It was observed that the asphalt mixtures that contain BFS as fine aggregate developed higher indirect tensile resistance (under dry and wet conditions) and was more resistant to moisture damage (greater TSR) with respect to that made with NGA. ANOVA analysis showed that the BFS had a significant effect on the dry and wet conditioned indirect tensile strength (Fig. 9).

Conclusions

The following conclusions can be taken specifically for the BFS analyzed. Similar studies using other types of BFS must be performed to verify what types of slags can be used to replace the fine fraction of NGA. Based on the results obtained, the following were concluded:

1. The best performance under monotonic and cyclic loads, and best resistance to moisture damage was attained by the mixture for which the finer fractions (smaller than 0.18 mm) of NGA was replaced by BFS in a ratio BFS = 12.5%.
2. When using fine granular aggregate substitution of BFS = 12.5%, the asphalt content in the mixture should be increased by only 0.25% to achieve an increase in the S/F ratio of 320 N/mm and an increase of 117 and 269 kPa in the wet and dry indirect tensile resistance, respectively, with respect to the control mixture. It was also observed an increment of the resilient modulus by 24, 25, and 75% for test temperatures of 10, 20, and 30°, resulting in higher resistance to permanent deformation. Besides, the resistance to fatigue under controlled stress loading also increased.
3. The ANOVA analysis showed that the BFS used as fine aggregate had a significant effect on the dynamic properties (resilient modulus, permanent deformation, and fatigue resistance) of hot mix asphalts and on their indirect tensile strength under wet conditions.
4. When fine particles of BFS analyzed were mixed with the asphalt, it helped to increase the stiffness of the asphalt mixture generating greater resistance to permanent deformation. Besides, it was responsible for providing higher cohesion, associated with the resistance to fatigue, and better adhesion between the binder and the aggregate associate to resistance in indirect tensile tests.
5. Based on the mineralogical and chemical compositions of the BSF, it was supposed that the asphalt that adhered to the fine aggregate fraction composed of BFS generated a material with better adhesion properties, compared to those using the aggregate composed of NGA. Adhesion properties were associated mainly with the content of CaO in the BFS. The content of SiO_2 (material with high mechanical strength and hardness) in the BFS also suggested that it could develop good cohesion properties.

References

AASHTO. 1991a. *Standard method of test for resistance to degradation of small-size coarse aggregate by abrasion and impact in the Los Angeles machine*. AASHTO T96. Washington, DC: AASHTO.

AASHTO. 1991b. *Standard method of test for specific gravity and absorption of coarse aggregate*. AASHTO T85. Washington, DC: AASHTO.

AASHTO. 2000. *Standard method of test for specific gravity and absorption of fine aggregate*. AASHTO T84. Washington, DC: AASHTO.

AASHTO. 2002. *Standard method of test for plastic fines in graded aggregates and soils by use of the sand equivalent test*. AASHTO T176. Washington, DC: AASHTO.

AASHTO. 2004. *Standard method of test for specific gravity of semi-solid asphalt materials*. AASHTO T228. Washington, DC: AASHTO.

AASHTO. 2005. *Standard method of test for resistance of coarse aggregate to degradation by abrasion in the Micro-Deval apparatus*. AASHTO T327. Washington, DC: AASHTO.

AASHTO. 2013. *Standard method of test for viscosity determination of asphalt binder using rotational viscometer*. AASHTO T316. Washington, DC: AASHTO.

AASHTO. 2015a. *Standard method of test for resistance to plastic flow of bituminous mixtures using Marshall apparatus*. AASHTO T245. Washington, DC: AASHTO.

AASHTO. 2015b. *Standard test method for organic impurities in fine aggregates for concrete*. AASHTO T21. Washington, DC: AASHTO.

Abu-Eishah, S. I., A. S. El-Dieb, and M. S. Bedir. 2012. "Performance of concrete mixtures made with electric arc furnace (EAF) steel slag aggregate produced in the Arabian Gulf region." *Constr. Build. Mater.* 34: 249–256. https://doi.org/10.1016/j.conbuildmat.2012.02.012.

AENOR (Norma Técnica Española). 2000. "Contenido de impurezas (agregado grueso) [Impurities content (coarse aggregate)]." UNE 14613. Madrid, Spain: AENOR.

Airey, G. D., A. C. Collop, and N. H. Thom. 2004. "Mechanical performance of asphalt mixtures incorporating slag and glass secondary aggregates." In *Proc., 8th Conf. Asphalt Pavements for Southern Africa (CAPSA'04)*. Pretoria, South Africa: CSIR Transportek, Asphalt Academy.

Akbarnejad, S., L. J. M. Houben, and A. A. A. Molenaar. 2014. "Application of aging methods to evaluate the long-term performance of road bases containing blast furnace slag materials." *Road Mater. Pavement Des.* 15 (3): 488–506. https://doi.org/10.1080/14680629.2014.907196.

Al-Hdabi, A., and H. Al Nageim. 2017. "Improving asphalt emulsion mixtures properties containing cementitious filler by adding GGBS." *J. Mater. Civ. Eng.* 29 (5): 04016297. https://doi.org/10.1061/(ASCE)MT.1943-5533.0001859.

Anderson, D. A., and W. H. Goetz. 1973. "Mechanical behavior and reinforcement of mineral filler-asphalt mixtures." *Proc. Assoc. Asphalt Paving Technol.* 42: 37–66.

ASA (Australasian Slag Association). 2002. *A guide to the use of iron and steel slag in roads*. Sydney, Australia: ASA.

ASTM. 1995. *Standard test method for softening point of bitumen (ring-and-ball apparatus)*. ASTM D36. West Conshohocken, PA: ASTM.

ASTM. 1999. *Standard test method for ductility of bituminous materials*. ASTM D-113. West Conshohocken, PA: ASTM.

ASTM. 2000. *Standard test methods for liquid limit, plastic limit, and plasticity index of soils*. ASTM D4318. West Conshohocken, PA: ASTM.

ASTM. 2001. *Standard test method for determining the percentage of fractured particles in coarse aggregate*. ASTM D5821. West Conshohocken, PA: ASTM.

ASTM. 2006. *Standard test method for softening point of bitumen (ring-and-ball apparatus)*. ASTM D36. West Conshohocken, PA: ASTM.

ASTM. 2009. *Standard test method for preparation and determination of the relative density of hot mix asphalt (HMA) specimens by means of the superpave gyratory compactor.* ASTM D6925. West Conshohocken, PA: ASTM.

ASTM. 2012. *Standard test method for effect of heat and air on a moving film of asphalt (rolling thin-film oven test)*. ASTM D2872-12e1. West Conshohocken, PA: ASTM.

ASTM. 2013. *Standard test method for penetration of bituminous materials*. ASTM D5/D5M. West Conshohocken, PA: ASTM.

ASTM. 2014. *Standard test method for effect of moisture on asphalt concrete paving mixtures*. ASTM D4867/D4867M. West Conshohocken, PA: ASTM.

ASTM. 2015. *Standard test method for viscosity determination of asphalt at elevated temperatures using a rotational viscometer*. ASTM D4402/D4402M. West Conshohocken, PA: ASTM.

ASTM. 2017a. *Standard test method for bulk specific gravity and density of non-absorptive compacted asphalt mixtures*. ASTM D2726/D2726M. West Conshohocken, PA: ASTM.

ASTM. 2017b. *Standard test method for indirect tensile (IDT) strength of asphalt mixtures*. ASTM D6931. West Conshohocken, PA: ASTM.

Beckhoff, B., B. Kanngießer, N. Langhoff, R. Wedell, and H. Wolff. 2006. *Handbook of practical X-ray fluorescence analysis*. New York, NY: Springer.

BSI (British Standards Institution). 2000. *Bituminous mixtures test methods for hot mix asphalt. Part 25: Cyclic compression test*. BS EN 12697-25. London: BSI.

BSI (British Standards Institution). 2005a. *Bituminous mixtures test methods for hot mix asphalt. Part 24: Resistance to fatigue*. BS EN 12697-24. London: BSI.

BSI (British Standards Institution). 2005b. *Bituminous mixtures test methods for hot mix asphalt. Part 26: Stiffness*. BS EN 12697-26. London: BSI.

Cheng, Y., J. Tao, Y. Jiao, Q. Guo, and C. Li. 2015. "Influence of diatomite and mineral powder on thermal oxidative ageing properties of asphalt." *Adv. Mater. Sci. Eng.* 2015: 1–10. https://doi.org/10.1155/2015/947834.

Cheng, Y., J. Tao, Y. Jiao, G. Tan, Q. Guo, S. Wang, and P. Ni. 2016. "Influence of the properties of filler on high and medium temperature performances of asphalt mastic." *Constr. Build. Mater.* 118: 268–275. https://doi.org/10.1016/j.conbuildmat.2016.05.041.

Chipera, S., and D. Bish. 2001. "Baseline studies of The Clay Minerals Society source clays: Powder X-ray diffraction analysis." *Clays and Clay Miner.* 49 (5): 398–409. https://doi.org/10.1346/CCMN.2001.0490507.

Dan, L., Z. Chuanfeng, Q. Yong, B. Heng, L. Keyao, and H. Junfei. 2014. "Analysing the effects of the mesoscopic characteristics of mineral powder fillers on the cohesive strength of asphalt mortars at low temperatures." *Constr. Build. Mater.* 65: 330–337. https://doi.org/10.1016/j.conbuildmat.2014.04.123.

Das, B., S. Prakash, P. S. R. Reddy, and V. N. Misra. 2007. "An overview of utilization of slag and sludge from steel industries." *Resour. Conserv. Recycl.* 50 (1): 40–57. https://doi.org/10.1016/j.resconrec.2006.05.008.

Davis, C., and C. Castorena. 2015. "Implications of physico-chemical interactions in asphalt mastics on asphalt microstructure." *Constr. Build. Mater.* 94: 83–89. https://doi.org/10.1016/j.conbuildmat.2015.06.026.

DNER (Departamento Nacional de Estradas de Rodagem). 1998. *Avaliação da resistência mecânica pelo método dos 10% de finos [Evaluation of mechanical resistance to coarse aggregate using 10% method]*. DNER-ME 096. Rio de Janeiro, Brazil: Departamento Nacional de Infraestrutura de Transporte.

Emery, J. J. 1982. "Slag utilization in pavement construction." In *Extending aggregate resources*, 95–118. Philadelphia, PA: ASTM.

FHWA (Federal Highway Administration Research and Technology). 2008. *Coordinating, developing, and delivering highway transportation innovations: User guidelines for waste and byproduct materials in pavement construction*. Rep. Publication Number: FHWA-RD-97-148. Washington, DC: FHWA.

Geiseler, J. 1996. "Use of steelworks slag in Europe." *Waste Manage.* 16 (1–3): 59–63. https://doi.org/10.1016/S0956-053X(96)00070-0.

Guo, M., Y. Tan, A. Bhasin, J. Wei, X. Yang, and Y. Hou. 2016. "Using molecular dynamics to investigate interfacial adhesion between asphalt binder and mineral aggregate." In *Proc., 4th Chinese-European Workshop on Functional Pavement Design (4th CEW 2016)*, edited by S. Erkens, X. Liu, K. Anupam, and Y. Tan, 517–527. Delft, Netherlands: Taylor & Francis Group.

HERALDO. 2016. "Colombia aumentó en 2015 la producción de hierro, oro y esmeraldas [Colombia increased the production of iron, gold and emeralds in 2015]." Accessed November 17, 2017. https://www.elheraldo.co/economia/colombia-aumento-en-2015-la-produccion-de-hierro-oro-y-esmeraldas-243818.

Houben, L. J. M., S. Akbarnejad, and A. A. A. Molenaar. 2010. "Performance of pavements with blast furnace base courses." In *Proc.,* *GeoShanghai 2010 Int. Conf. on Paving Materials and Pavement Analysis Geotechnical*, 476–483. Reston, VA: ASCE.

INVIAS (Instituto Nacional de Vías). 2013. *Especificaciones generales de construcción de carreteras*. Bogotá, Colombia: INVIAS.

Jones, D. E. 1982. "Application of steel plant by-products to roadworks." In *Proc., Conf. Australian Road Research Board*. Melbourne, Australia: ARRB Group Limited.

Kuity, A., and A. Das. 2015. "Homogeneity of filler distribution within asphalt mix – A microscopic study." *Constr. Build. Mater.* 95: 497–505. https://doi.org/10.1016/j.conbuildmat.2015.07.043.

León, N. A., N. R. Rojas, B. U. Suárez, and O. Bustamante. 2009. "Evaluación experimental de unidades sílico-calcáreas a partir de escoria de alto horno y cal hidráulica para mampostería [Experimental evaluation of silicon-calcareous units from blast furnace slag and hydraulic lime for masonry]." *Dyna* 76 (160): 247–254.

Li, C., Z. Chen, S. Wu, B. Li, J. Xie, and Y. Xiao. 2017. "Effects of steel slag fillers on the rheological properties of asphalt mastic." *Constr. Build. Mater.* 145 (1): 383–391. https://doi.org/10.1016/j.conbuildmat.2017.04.034.

Li, R., H. Du, Z. Fan, and J. Pei. 2016. "Molecular dynamics simulation to investigate the interaction of asphaltene and oxide in aggregate." *Adv. Mater. Sci. Eng.* 2016: 1–10. https://doi.org/10.1155/2016/3817123.

Liao, M. C., and J. S. Chen. 2011. "Zero shear viscosity of bitumen-filler mastics." *J. Mater. Civ. Eng.* 23 (12): 1672–1680. https://doi.org/10.1061/(ASCE)MT.1943-5533.0000331.

Marriaga, J. L., and P. Claisse. 2011. "The influence of the blast furnace slag replacement on chloride penetration in concrete." *Ingeniería e Investigación* 31 (2): 38–47.

Misra, A., D. Biswas, and S. Upadhyaya. 2005. "Physico-mechanical behavior of self cementing class C fly ash-clay mixtures." *Fuel* 84 (11): 1410–1422. https://doi.org/10.1016/j.fuel.2004.10.018.

Modarres, A., and M. Rahmanzadeh. 2014. "Application of coal waste powder as filler in hot mix asphalt." *Constr. Build. Mater.* 66: 476–483. https://doi.org/10.1016/j.conbuildmat.2014.06.002.

Moore, D., and R. Reynolds. 1997. *X-Ray diffraction and the identification and analysis of clay minerals*. 2nd ed. New York: Oxford University Press.

Muniandy, R., E. Aburkaba, and L. Mahdi. 2013. "Effect of mineral filler type and particle size on asphalt-filler mastic and stone mastic asphalt laboratory measured properties." *Aust. J. Basic Appl. Sci.* 7 (11): 475–487.

Nassar, A. I., M. K. Mohammed, N. Thom, and T. Parry. 2016. "Mechanical, durability and microstructure properties of cold asphalt emulsion mixtures with different types of filler." *Constr. Build. Mater.* 114: 352–363. https://doi.org/10.1016/j.conbuildmat.2016.03.112.

NLT (Norma Laboratorio de Transporte). 1991. *Standard method for the determination of the flakiness index of the aggregate*. NLT 354. Madrid, Spain: Centro de Estudios y Experimentación de Obras Públicas.

Normas NLT. 1988. *Método para determinar la variación de la consistencia del betún asfáltico con los cambios de temperatura (susceptibilidad) [Method to determine the variation in the consistency of asphalt bitumen with temperature changes (susceptibility)]*. NLT 181. Madrid, Spain: Normas NLT.

Noureldin, A. S., and R. S. McDaniel. 1990. "Evaluation of surface mixtures of steel slag and asphalt." *Transp. Res. Rec.* 1269: 133–149.

Nouvion, S., A. Jullien, M. Sommier, and V. Basuyau. 2009. "Environmental modeling of blast furnace slag aggregate production." *Road Mater. Pavement Des.* 10 (4): 715–745. https://doi.org/10.3166/rmpd.10.715-745.

NSA (National Slag Association). 2006. "Blast furnace slag." Accessed April 11, 2016. http://nationalslag.org/blast-furnace-slag.

Okumura, H. 2013. "Recycling of iron and steelmaking slags in Japan." In *Proc., 1st Int. Conf. on Processing Materials for Properties*, 803–806. Warrendale, PA: Minerals, Metals, and Materials Society (TMS).

Proctor, D. M., K. A. Fehling, E. C. Shay, J. L. Wittenborn, C. Avent, R. D. Bigham, M. Connolly, B. Lee, T. O. Shepker, and M. A. Zak. 2000. "Physical and chemical characteristics of blast furnace, basic oxygen furnace, and electric arc furnace steel industry slags." *Environ. Sci. Technol.* 34 (8): 1576–1582. https://doi.org/10.1021/es9906002.

Reed, S. J. B. 2005. *Electron microprobe analysis and scanning electron microscopy in geology.* Cambridge, UK: Univ. of Cambridge.

Shen, H., and E. Forssberg. 2003. "An overview of recovery of metals from slags." *Waste Manage.* 23 (10): 933–949. https://doi.org/10.1016/S0956-053X(02)00164-2.

Shi, C. 2004. "Steel slag—Its production, processing, characteristics, and cementitious properties." *J. Mater. Civ. Eng.* 16 (3): 230–236. https://doi.org/10.1061/(ASCE)0899-1561(2004)16:3(230).

Sorlini, S., A. Sanzeni, and L. Rondi. 2012. "Reuse of steel slag in bituminous paving mixtures." *J. Hazard. Mater.* 209–210: 84–91. https://doi.org/10.1016/j.jhazmat.2011.12.066.

Tenza-Abril, A. J., J. M. Saval, and A. Cuenca. 2015. "Using sewage-sludge ash as filler in bituminous mixes." *J. Mater. Civ. Eng.* 27 (4): 04014141. https://doi.org/10.1061/(ASCE)MT.1943-5533.0001087.

Transport Roads and Maritime Services. 2012. *Test method T220 Iron unsoundness in metallurgical slag*. T220 (RMS 12.495). Camperdown, NSW, Australia: Transport Roads and Maritime Services.

Ucrós, J. C. 2009. "Propuesta para la implementación de instrumentos de política ambiental en la planta siderúrgica de Acerías Paz del Río S.A. [Proposal for the implementation of environmental policy instruments in the steel plant Acerías Paz del Río S.A.]." M.S. thesis, Pontificia Universidad Javeriana.

UPME (Unidad de Planeación Minero Energética). 2014. *Indicadores de la minería en Colombia [Indicators of mining in Colombia]*. Bogotá, Colombia: UPME.

Van Oss, H. G. 2003. *Slag-iron and steel*, 69.1–69.7. Reston, VA: US Geologycal Survey.

Veytskin, Y., C. Bobko, C. Castorena, and R. Kim. 2015. "Nanoindentation investigation of asphalt binder and mastic cohesion." *Constr. Build. Mater.* 100: 163–171. https://doi.org/10.1016/j.conbuildmat.2015.09.053.

WSDOT (Washington State Department of Transportation). 2015. *Strategies regarding use of steel slag aggregate in pavements. A report to the state legislature in response to 2ESHB 1299*. Olympia, WA: Washington State DOT Construction Division Pavements Office.

Yiqiu, T., L. Xiaolin, and W. Jiantao. 2012. "Internal influence factors of asphalt-aggregate filler interactions based on rheological characteristics." *J. Mater. Civ. Eng.* 24 (12): 1520–1528. https://doi.org/10.1061/(ASCE)MT.1943-5533.0000506.

Zarei, Z., and M. B. Reza. 2015. "Application of iron slag at different pavement layers." *J. Environ. Treat. Technol.* 3 (3): 158–162.

Zhang, G., J. Germaine, M. Torrence, and A. A. Whittle. 2003. "A simple sample-mounting method for random powder X-ray diffraction." *Clays Clay Miner.* 51 (2): 218–225. https://doi.org/10.1346/CCMN.2003.0510212.